Received: 24 May 2024 | Revised: 4 July 2024 | Accepted: 23 July 2024

DOI: 10.1096/fj.202401165R

The FASEB Journal

RESEARCH ARTICLE

Activation of the G protein-coupled sulfakinin receptor inhibits blood meal intake in the mosquito *Aedes aegypti*

Linlong Jiang[1,2] | **Xiao Bing Xie**[3] | **Lei Zhang**[1,2,4] | **Yu Tang**[1,2] | **Xiaojing Zhu**[1,2] | **Yuqi Huang**[1,2] | **Yue Hong**[2] | **Bill S. Hansson**[5] | **Zong Jie Cui**[3] | **Qian Han**[1,2,4]

[1]Laboratory of Tropical Veterinary Medicine and Vector Biology, School of Life Sciences, Hainan University, Haikou, Hainan, China

[2]Hainan Province Key Laboratory of One Health, Collaborative Innovation Center of One Health, Hainan University, Haikou, Hainan, China

[3]College of Life Sciences, Beijing Normal University, Beijing, China

[4]Hainan International One Health Institute, Hainan University, Haikou, Hainan, China

[5]Department of Evolutionary Neuroethology, Max Planck Institute for Chemical Ecology, Jena, Germany

Correspondence
Zong Jie Cui, College of Life Sciences, Beijing Normal University, Beijing 100875, China.
Email: zjcui@bnu.edu.cn

Qian Han, School of Life Sciences, Hainan University, Haikou, Hainan, China.
Email: qianhan@hainanu.edu.cn

Funding information
The National Natural Science Foundation of China, Grant/Award

Abstract

Little is known about the blood-feeding physiology of arbovirus vector *Aedes aegypti* although this type of mosquito is known to transmit infectious diseases dengue, Zika, yellow fever, and chikungunya. Blood feeding in the female *A. aegypti* mosquito is essential for egg maturation and for transmission of disease agents between human subjects. Here, we identify the *A. aegypti* sulfakinin receptor gene *SKR* from the *A. aegypti* genome and show that *SKR* is expressed at different developmental stages and in varied anatomical localizations in the adult mosquito (at three days after eclosion), with particularly high expression in the CNS. Knockingdown sulfakinin and sulfakinin receptor gene expression in the female *A. aegypti* results in increased blood meal intake, but microinjection in the thorax of the sulfakinin peptide 1 and 2 both inhibits dose dependently blood meal intake (and delays the time course of blood intake), which is reversible with receptor antagonist. Sulfakinin receptor expressed ectopically in mammalian cells CHO-K1 responds to sulfakinin stimulation with persistent calcium spikes, blockable with receptor antagonist. These data together suggest that activation of the Gq protein-coupled (i.e., calcium-mobilizing) sulfakinin receptor inhibits blood meal intake in female *A. aegypti* mosquitoes and could serve as a strategic node for the future control of *A. aegypti* mosquito reproduction/population and disease transmission.

KEYWORDS

blood meal intake, Ca^{2+} oscillations, disease transmission, mosquito control, satiety regulation, sulfakinin, sulfakinin receptor

Abbreviations: BSA, bovine serum albumin; CCD, charge coupled device; CCK, cholecystokinin; CCK1R, cholecystokinin 1 receptor; DAPI, 4',6-diamidino-2-phenylindole; DEPC, diethylpyrocarbonate; DMEM, Dulbecco's modified Eagle's medium; dsRNA, double stranded RNA; EC50, concentration at which 50% of maximum effect can be obtained; FBS, fetal bovine serum; GFP, green fluorescent protein; GPCR, Gq protein-coupled receptor; HEPES, 4-(2-hydroxyethyl)-1-piperazine-ethane-sulfonic acid; MEM, minimum essential medium; qPCR, quantitative real-time PCR; RNAi, RNA interference; RPS17, ribosomal protein S17; RRID, research resource identifier; SEM, standard error of means; SK, sulfakinin; SK1, sulfakinin 1; SK2, sulfakinin 2; SKR, sulfakinin receptor.

Linlong Jiang and Xiao Bing Xie should be considered joint first authors.

Zong Jie Cui and Qian Han should be considered joint senior authors.

Number: 32271278, U22A20363 and 31971170; Hainan Province Science and Technology Special Fund, Grant/Award Number: ZDKJ2021035; National High-end Foreign Experts Recruitment Plan, Grant/Award Number: G2021034003L

1 | INTRODUCTION

The dengue, Zika, yellow fever, and chikungunya virus vector, the mosquito *Aedes aegypti*, is now present in expanding areas of the world.[1] Current mosquito control methods are impeded by non-specificity and insecticide (organochlorines, organophosphates, carbamates, and pyrethroids) resistance.[2–4] Thus, it is imperative to develop insecticides targeting specific physiology of the *Aedes aegypti* mosquito, with decreased off-target effects.

A. aegypti female mosquitos need a blood meal to produce eggs, but with some exception.[5,6] Early oogenesis is initiated after a blood meal, to stimulate a single layer of the follicular epithelial cells surrounding the oocyte to secret eggshell proteins, in preparation for eventual oviposition.[7,8] Blood meal intake has been found to be essential for the deposition of eggshell proteins including enzymes for eggshell melanization, protein cross-linking, and sclerotization, to protect the laid eggs against environmental stress and desiccation.[7–9] The expression of the eggshell protein Nudel (a serine protease), for example, has been found to be upregulated 200-fold transiently after a blood meal, to help promote subsequent eggshell maturation and egg survival.[7] Further, the dengue, Zika, yellow fever, and chikungunya viruses are transmitted by *A. aegypti* female mosquitos between human subjects by the process of blood feeding.[2] Therefore, elucidation of the cellular and molecular regulatory mechanisms of blood meal intake of *A. aegypti* would provide potentially two critical targeting strategies for mosquito control and prevention of disease transmission: suppressed mosquito reproduction and reduced virus transmission. In the present work, we focused on the possibility of sulfakinin receptor regulation of blood meal intake by *A. aegypti*.

The insect peptide sulfakinin (SK) is found in multiple insect species such as *Blattella germanica*, *Bombyx mori*, *Locusta migratoria*, *Drosophila melanogaster*, and *Nilaparvata lugens*,[10–14] where it is known to regulate food intake, digestive enzyme secretion,[15–17] nociception,[18] learning and memory,[19] development, and reproduction.[15,20–24] In the cockroach *Leucophaea maderae*, SK also displayed myotrophic effects.[25,26]

The SK gene *DSK* was first cloned from *D. melanogaster*[27] as an invertebrate homolog of the vertebrate cholecystokinin (CCK).[28] In *D. melanogaster*, SK not only inhibits food intake but also regulates mating, aggression, and stress.[29–31]

To date, only limited works have been done to elucidate the function of SK receptors (SKR) in the context of insect food intake. Two SKR receptors have been found in the CNS of *Rhodnius prolixus*, where interference of their expression was found to increase blood intake.[32] SKR receptors cloned from *Bombyx mori* were found primarily coupled to Gq protein and therefore to calcium signaling, to regulate food intake in silkworms.[12] Therefore, SK and SKR regulate food intake in species such as *Gryllus bimaculatus*,[23] *Tribolium castaneum*, and *Tenebrio molitor*,[21,24] downregulated expression of SK and their receptors all led to increases in food consumption. But whether SK or SKR would play any physiological role in the medically important mosquito *A. aegypti*, however, has not been studied.

In the present work, we aimed to identify the *SK* and *SKR* genes from the genome of *A. aegypti*, to analyze their anatomical and developmental transcriptional patterns. RNA interference (RNAi) was used in adult females to examine effect of knockdown of *SK* and *SKR* gene expression on blood meal intake. The effect of microinjected SK 1 and 2 on blood meal intake, as well as the possible reversal by SKR receptor antagonist were examined. *SKR* gene was ectopically expressed in the mammalian cell line CHO-K1 to check, by Fura-2 fluorescence calcium imaging, the possible coupling of SKR activation to Gq protein and therefore calcium signaling.

2 | MATERIALS AND METHODS

2.1 | Materials

Dulbecco's Modified Eagle's Medium (DMEM)/F12 medium (#C11330500BT) and fetal bovine serum (FBS) (#10099141) were bought from Thermo Scientific (Shanghai, China). 4-(2-Hydroxyethyl)-1-piperazine-ethanesulfonic acid (HEPES) (#391338) was from Calbiochem (Darmstadt, Germany). The sulfated cholecystokinin octapeptide (CCK) (#1166) was from Tocris Cookson (Bristol, UK). The SK peptides SK1 (#P27064-1) and SK2 (#P27064-2) were from Sangon Biotech (Shanghai, China). Minimum essential medium (MEM) amino acids mixture (50×, #11130-051) and 0.25% Trypsin–EDTA (#52500056) were from Gibco™ (Shanghai, China). Dopamine (#H8502), collagenase P (#11213873001),

paraformaldehyde (#P6148), and soybean trypsin inhibitor (#T9128) were from Sigma-Aldrich (Shanghai, China). Fura-2 AM (#1051B) was from Dakewe (Beijing, China). JetPRIME transfection reagent (#101000046) was from PolyPlus-transfection (New York, USA). Cell-Tak (#354241) was from BD Biosciences (Bedford, MA, USA). Matrix-Gel (C-0372) was from Beyotime (Shanghai, China). Ampicillin (#B11601) and kanamycin (#CW0608) were from CWBio (Beijing, China). Mounting medium, antifade (with DAPI) (#S2110), and bovine serum albumin V (BSA) (#A8020) were from Solarbio (Beijing, China). Penicillin/streptomycin solution (SV30010) was from Hyclone™ (Shanghai, China).

2.2 | Mosquito rearing

The wild-type *A. aegypti* Rockefeller strain was reared at 24–27°C with 70% relative humidity in The Insectary at Hainan University. Larvae were fed with fish food ad libitum. Adults were maintained on an 8% (8 g /100 mL) sucrose source under a 16 h (light): 8 h (dark) light cycle as reported before.[33]

2.3 | Quantitative real-time PCR

To verify the expression patterns of SK gene *SK* (AAEL006451) and SK receptor gene *SKR* (AAEL017238) at different life stages, and in different tissues in female (head, legs, thorax, midgut, cuticle, salivary glands, and ovary) or male (head, legs, thorax, midgut, cuticle) adults three days after eclosion ($n = 50–80$), quantitative real-time PCR (qPCR) was performed. The primers of SK qPCR were forward: 5′-GAC AGT GGT TAG AGC-3′ and reverse: 5′-ACT TTG CAA TTT GTT CAG TCC-3′ (exon 1). The qPCR primers of SKR were forward: 5′-GTG GAT TCT ACA TGG TGC TTC C-3′ and reverse: 5′-CGA AGT CGT GCA TCC C-3′ (exon 3). RNA isolation and cDNA synthesis were done using TRIzol reagent (Invitrogen, California, USA) and PrimeScipt™ RT reagent kit including gDNA eraser (TaKaRa, Kusatsu, Japan), respectively. The synthesized cDNA was stored at −20°C until use.

qPCR reactions were performed in a LightCycler 96 (Roche, Mannheim, Germany) using SYBR green Master I (Roche), with the following conditions: initial denaturation at 95°C for 600 s, followed by 40 cycles at 95°C for 10 s, 55°C for 10 s, and 72°C for 10 s. The gene expression experiments were carried out in three replicates and four technical replicates for each group of cDNA samples. *A. aegypti* ribosomal protein S17 gene *RPS17* (AAEL025999) (forward: 5′-AAG AAG TGG CCA TCA TTC CA-3′ and reverse: 5′-GGT CTC CGG GTC GAC TTC-3′) was used as internal control. Relative quantification was analyzed by $2^{-\Delta\Delta Ct}$ method.[34]

2.4 | Double-stranded RNA synthesis and injection for gene knockdown

Double-stranded RNA (dsRNA) primers for SK gene *SK* and SK receptor gene *SKR* were designed (T7 RiboMAX™ Express RNAi System). The single-strand template was first synthesized by PCR amplification, and the complete dsRNA was then synthesized in vitro (T7 RiboMAX™ Express RNAi System) (Promega, Beijing, China). The initial and final purifications were carried out according to the manufacturer's manual. Synthesized dsRNA was kept at −80°C until use. The PCR amplification primers for SK were forward 1:5′-GGA TCC taa tac gac tca cta tag ggG TAA TTC ACA ATC CAC CAG G-3′ (lower case indicates T7 promoter sequence), forward 2:5′-GTA ATT CAC AAT CCA CCA GG-3′, and reverse 1:5′-TTA CCG TCT TCC GAA TCT CA-3′, and reverse 2:5′-GGA TCC taa tac gac tca cta tag ggT TAC CGT CTT CCG AAT CTC A-3′. The PCR amplification primers for SKR were forward 1:5′-GGA TCC taa tac gac tca cta tag ggG GTG CGG CAG TCT GTT CT-3′, forward 2:5′-GGT GCG GCA GTC TGT TCT-3′ and reverse 1:5′-TAT TGT TGT TAT GGC GAC GG-3′, reverse 2:5′-GGA TCC taa tac gac tca cta tag ggT ATT GTT GTT ATG GCG ACG G-3′. The primers of green fluorescent protein as a negative control were forward 1:5′-GGA TCC taa tac gac tca cta tag ggC ACA TGA AGC AGC ACG ACT T-3′, forward 2:5′-CAC ATG AAG CAG CAC GAC TT-3′ and reverse 1:5′-GGG TGT TCT GCT GGT AGT GG-3′, reverse 2:5′-GGA TCC taa tac gac tca cta tag ggG GGT GTT CTG CTG GTA GTG G-3′.

Female adult mosquitoes (three days after eclosion) were exposed to cold anesthesia at −20°C for 2–3 min, and then transferred on ice for dsRNA injection. Mosquitoes from the same batch were used in parallel experiments: *GFP* dsRNA (4392 ng/μL) control, DEPC (diethylpyrocarbonate-treated) water control, *SK* dsRNA (4198 ng/μL), and *SKR* dsRNA (4237 ng/μL), with 40 mosquitoes per group. Approximately, 1 μL dsRNA was injected into the thorax of each female adult, via glass capillary tube (tip diameter 3 μm). After weighing and blood-feeding experiments, head tissues from 10 mosquitos were placed in a test tube, with each group using three tubes. Changes in gene expression were detected through qPCR, as described before.[35]

2.5 | Synthesis and microinjection of SK1 and SK2

The SK gene *SK* encodes a prepropeptide containing two SK peptide sequences in *A. aegypti*: SK1—FDDY(SO_3H)

GHMRF and SK2—GGEGEQFDDY(SO_3H)GHMRF. Both peptides were synthesized commercially: SK1 at purity of 98.10% and SK2 at 98.19% (Sangon Biotech, Shanghai, China). A total of 120 female adult mosquitoes (3 days after eclosion) were divided into four experimental groups: DEPC water, SK1, SK1 + SK2, and SK2, with 30 in each group. Each peptide (200 pmol/μL, 1 μL) was injected into the thorax region of adult mosquito.

Samples were taken immediately after weighing and blood-feeding experiment. Ten mosquitoes were put in one tube, three tubes were used for each group. Mosquito heads were excised after cold anesthesia and used for RNA extraction and cDNA synthesis. Reverse transcribed cDNA was used as template to detect changes in gene expression by qPCR.

2.6 | Injection of different SK2 doses and reversal by antagonist proglumide

Different concentrations of SK2 peptides were injected into female mosquitoes. A total of 120 female adult mosquitoes (three days after eclosion) were divided into four experimental groups: DEPC water, SK2 at 50 μM (50 pmol/μL, 1 μL), SK2 at 100 μM (100 pmol/μL, 1 μL), and SK2 at 150 μM (150 pmol/μL, 1 μL), with 30 in each group. Twenty-four (24) hours after injection, a blood meal weighing experiment was conducted. Afterward, SK2 at 200 μM (200 pmol/μL) was mixed 1:1 with the cholecystokinin antagonist proglumide 28 mM (28.06 nmol/μL) (SK2 at 100 μM, proglumide 14 mM), and each mosquito was injected with 1 μL. Twenty-four (24) hours later, a blood meal weighing experiment was conducted to analyze the changes in blood meal weight.

2.7 | Blood meal size measurements of fed mosquitoes

The blood meal size of female adult mosquitoes (three days after eclosion) with uniform size and good flight status was measured. Mosquitoes were starved for 12 h before injection, and then continued to starve for 24 h more, before blood meal; mosquitoes were weighed (balance: model BCE124I-1CCN, sartorius.com.cn) both immediately before and after blood meal, and the amount of blood intake was calculated for each mosquito (blood intake = weight of mosquitoes after the blood meal—weight of mosquitoes before the blood meal) (illustrated below). The simple criterion for the completion of a blood meal is that the mosquito stops at a place to no longer move actively, as reported before.[36]

Eighty (80) female mosquitoes were divided into four groups, and each group was placed in a separate cage for 24 h: DEPC water control, SK1, SK1 + SK2, and SK2. The number of mosquitoes having completed a full blood meal was recorded every 10 min until all mosquitoes had done so. These experiments were repeated three times.

2.8 | SK receptor gene *SKR* and *KillerRed-SKR* constructs

The complete SKR coding sequence *SKR* was synthesized de novo at Genescript (Nanjing, China). The gene sequence was inserted into *pcDNA3.1*$^{(+)}$ vector to get *pSKR-cDNA3.1*$^{(+)}$. The red fluorescent protein sequence *pKillerRed* was tagged to 5′ end of *SKR* sequence, to obtain plasmid *pKillerRed-SKR* (Genescript, Nanjing, China).

2.9 | Functional expression of SK receptor gene *SKR* in CHO-K1 cells

Chinese hamster ovary cells K1 strain (CHO-K1) (RRID:CVCL-0214) were purchased from the Shanghai Institute of Life Sciences Chinese Academy of Sciences and cultured in DMEM/F12 high glucose medium containing 10% FBS and 1% penicillin/streptomycin solution,

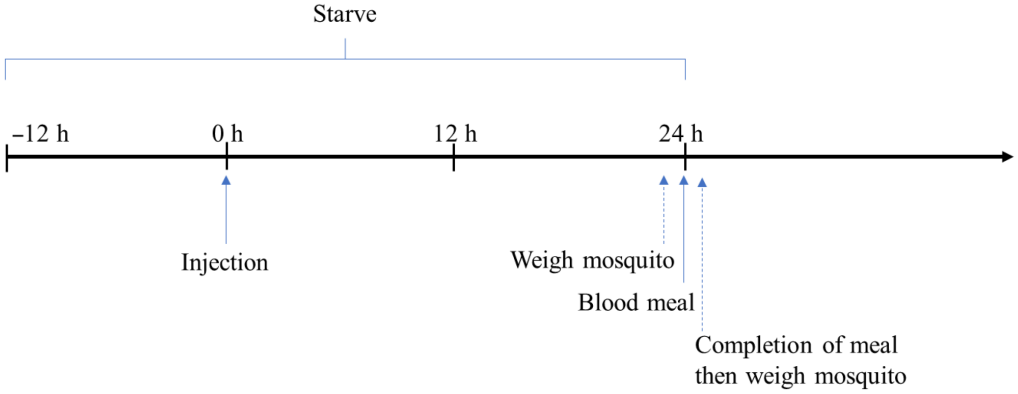

in 25 cm^2 flasks in a CO_2 incubator (37°C, 5% CO_2/95% air).

CHO-K1 cells grown to 80%–90% confluency were used for *SKR* gene transfection. Medium was replaced with serum-free medium (4 mL), a mixture composed of jetPRIME buffer (400 μL), plasmid (6 μg), jetPRIME transfection reagent (12 μL) was added, and cultured for 24–36 h. CHO-K1 cells so transfected with plasmids *pSKR* and *pSKR-KillerRed* were named SKR-CHO-K1 and SKR-KillerRed-CHO-K1 cells, respectively.

2.10 | Isolation of rat pancreatic acini

Male Sprague–Dawley (RRID:RGD-70508) rats (250–450 g in body weight) were killed by asphyxia in 100% CO_2. The pancreas was excised, and rat pancreatic acini were isolated by collagenase P (0.2 g L^{-1}, 10 mL) digestion in a shaking water bath (37°C, 110 cycles per min). Collagenase digestion was for 2 × 10 min, with one change of fresh collagenase P-containing buffer in between, as reported.[37–39] This animal protocol was approved by the Animal Use and Ethics Committee, College for Life Sciences, Beijing Normal University (No. CLS-EAW-2017-015).

Buffer for rat pancreatic acini isolation was composed of (in mM): NaCl 118, KCl 4.7, $MgCl_2$ 1.13, $CaCl_2$ 2.5, NaH_2PO_4 1.0, D-glucose 5.5, 4-(2-hydroxyethyl)-1-piperazine ethanesulfonic acid (HEPES) 10, L-glutamine 2.0, bovine serum albumin (BSA) 2%, minimum essential medium (MEM) amino acids mixture 2%, soybean trypsin inhibitor 0.1 g L^{-1}, with pH adjusted to 7.4. Buffer used for perifusion and calcium imaging was the same but with the following omitted from the buffer: BSA, amino acid mixture, and trypsin inhibitor.

2.11 | Calcium imaging

Transfected SKR-CHO-K1 cells were harvested and loaded with the fluorescent indicator Fura-2 AM (10 μM) at 37°C in a shaking water bath for 50 min (37°C, 60 cycles per min). Fura-2-loaded cells were attached to Cell-Tak- or Matrix-Gel-coated coverslips at the bottom part of a Sykes-Moore perfusion chamber. The perfusion chamber was placed on the platform of an inverted fluorescent microscope (Nikon TE-2000 U) attached to a calcium imaging device (Photon Technology International—PTI, New Jersey, USA). Fura-2 was excited alternately at 340/380 nm with excitation light from DeltaRam X (PTI, New Jersey, USA). Emitted fluorescence images were captured on a CCD camera (NEO-5.5-CL-3) (Andor/Oxford Instruments, UK) (RRID:SCR-023609). Fluorescent ratios F_{340}/F_{380} obtained were indicative of cytosolic calcium concentration and plotted against time with SigmaPlot (RRID:003210). The original calcium tracings presented were each from an individual cell.

The freshly isolated rat pancreatic acini were similarly loaded with Fura-2 AM (10 μM, 30 min), attached to the bottom coverslip (coated with Cell-Tak or Matrix-Gel) of Sykes-Moore perfusion chambers for calcium imaging as reported previously.[40–42]

2.12 | Confocal imaging of sulfakinin receptor-KillerRed construct

SKR-KillerRed-CHO-K1 cells were fixed in 4% paraformaldehyde, counterstained with nuclear dye DAPI, and imaged in a laser scanning confocal microscope (Zeiss LSM 710) under objective 63×/1.40 oil: KillerRed: λ_{ex}, 561 nm, λ_{em} 618 nm; DAPI: λ_{ex} 405 nm, λ_{em} 477 nm.

2.13 | Data processing and analysis

qPCR data were normalized by internal reference gene (*A. aegypti* ribosomal protein S17 gene *RPS17*, accession No. AAEL025999), and the relative expression was calculated by $2^{-\Delta\Delta Ct}$ method. All experimental data were processed and analyzed with GraphPad Prism (RRID:SCR-002798) 8.4.0. *T*-test and one-way ANOVA were used for statistical significance. Level of significance: $^{*}p < .05$, $^{**}p < .01$, $^{***}p < .001$, $^{****}p < .0001$. In Figures 1 and 3, significant differences are marked with alphabets a–g, with the same letter indicating no significant difference, while different letters indicate significant differences. All data obtained from calcium imaging were presented in mean ± SEM. Student's *t*-test was used for statistical analysis, with a value of $p < .05$ taken as significant, as indicated by an asterisk (*).

3 | RESULTS

3.1 | Spatiotemporal expression of *SK* and *SKR* transcripts in *A. aegypti*

The spatiotemporal expression profiles of *SK* and *SKR* genes were analyzed with qPCR. The *SK* transcript was detected in *A. aegypti* from the egg stage, and eight different developmental stages (1st to 4th instar, white and black pupal stages, and adult) (Figure 1A). The highest expression

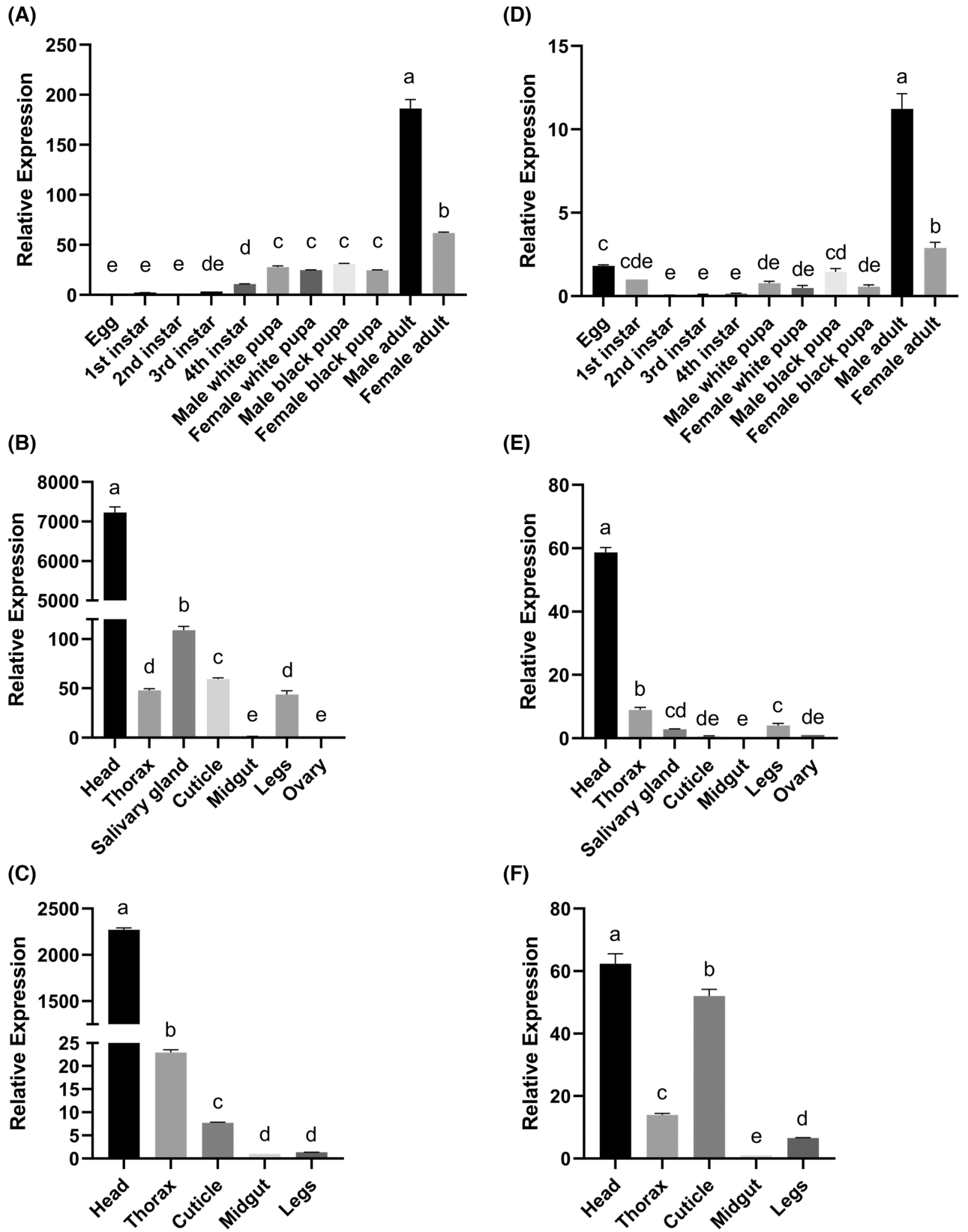

FIGURE 1 Spatiotemporal expression profiles of *SK and SKR* genes in *A. aegypti*. (A) The *SK* mRNA level in eight developmental stages from egg to adult. The *SK* mRNA levels in different tissues in female (B) and male (C) adults. (D) The *SKR* mRNA level of eight developmental stages from egg to adult. The *SKR* mRNA levels of different tissues in female (E) and male (F) adult mosquitoes. All data are presented as mean ± SEM. Small letters "a, b, c, d, e" within panels (A–F) denote that significant differences are marked with alphabet singlets a–e, or doublets, triplets with the same letter(s) or letter combinations indicating no significant difference, while different letters or combinations indicate significant differences.

level was found in adult male mosquitoes and the lowest in eggs (Figure 1A). *SK* expression in the adult mosquitos (three days after eclosion) was examined. Comparison of *SK* expression in the head, thorax, salivary glands, cuticle, midgut, legs, and the ovary of female mosquitoes revealed the highest expression level in the head, and lowest in the midgut and the ovary; in the head, it was 7228 times that of the ovary. Relatively high expression was found also in the salivary glands (Figure 1B). In male mosquitoes, a comparison of *SK* expression in the head, thorax, cuticle, midgut, and legs revealed the highest expression in the head and the lowest in the midgut, while a moderate expression was observed in the thorax (Figure 1C).

SKR transcript was detected at all developmental stages of *A. aegypti* (Figure 1D). *SKR* transcript expression was relatively low at the egg, larval, and pupal stages. After emergence, *SKR* expression increased significantly. The highest expression level was found in adult male mosquitoes (three days after eclosion) and lowest in second-instar larvae (Figure 1D). *SKR* expression was detected in all tissues in both male and female adult *A. aegypti* mosquitoes. In female mosquitoes, the highest expression was found in the head, and lowest in midgut (Figure 1E). In male adult mosquitoes, the highest expression levels were found in the head and cuticle and the lowest in the midgut (Figure 1F).

3.2 | *SK* and *SKR* gene knockdown increased the size of blood meals in adult mosquitoes

The SK peptides are known satiety factors to inhibit food intake in other insects. To investigate whether this is also the case in *A. aegypti*, *SK* and *SKR* gene expressions in starvation and after a blood meal were compared. Compared with starvation, six hours after a blood meal the abundance of *SK* and *SKR* mRNA in the mosquito head more than doubled and nearly quadrupled, respectively (Figure 2A). Therefore, we wondered whether the expressions of *SK* and *SKR* genes are involved in satiety regulation and blood meal intake in *A. aegypti*. *SK* and *SKR* gene known-down experiments were done to examine their effects on blood meal intake in female mosquitoes. The blood meal weight imbibed by *A. aegypti* was then measured for different treatments. No differences in body weight were noted among mosquitoes treated with diethylpyrocarbonate-treated (DEPC) water (as negative control 1), *dsGFP* (against the *GFP* gene which is not expressed in this work, as negative control 2), *dsSK*, or *dsSKR*, while the size of blood meals was significantly higher in *dsSK* and *dsSKR* treated mosquitoes when compared with DEPC water and *dsGFP* controls (Figure 2B).

The expression of *SK* and *SKR* genes in *A. aegypti* head was downregulated by RNA interference (RNAi) (Figure 2C,D). Thoracic injections of *dsSK*, *dsSKR*, *dsGFP*, or DEPC water were performed in adult mosquitoes. Female mosquitoes were fed a blood meal 24 hours after injection of dsRNA and mosquito heads were excised six hours after the blood meal for qPCR analysis. The relative expression of *dsSK* mRNA was significantly reduced (down to 40% of controls) when compared with DEPC water and *dsGFP* controls (left part, Figure 2C). *SK* mRNA also decreased markedly (down to 60% of controls) after *dsSKR* injection (right part, Figure 2C). The expression of *SKR* mRNA, however, did not change after *dsSK* RNA (left part, Figure 2D). The ds*SKR* interference experiment revealed that in comparison with controls (*dsGFP*, DEPC water), the relative expression of *SKR* mRNA was significantly reduced (down to 60% of controls) (right part, Figure 2D).

3.3 | SK microinjection decreased blood meal feeding in female mosquitoes

To verify data from the RNA interference experiments, female mosquitoes were injected with sulfakinin peptides, and effect on blood meal intake was examined. Both sulfakinin 1 [SK1—FDDY(SO_3H)GHMRF] and sulfakinin 2 [SK2—GGEGEQFDDY(SO_3H)GHMRF] were used for in vivo injection. A total of 120 female adult mosquitoes were randomly allocated into four groups: DEPC water, SK1, SK1 + SK2, and SK2. Twenty-four hours after SK injection, female mosquitoes were blood fed, immediately dissected and mosquito heads were used for qPCR analysis.

The size of blood meals post-SK injection is shown in Figure 3A. Adult mosquitoes showed similar body weights among the four groups, but blood meal size decreased markedly in the three SK-injected groups when compared with DEPC water control. The relative *SK* mRNA expression was also found to decrease significantly after SK injections when compared with DEPC water-injected controls. But no difference was found among the three SK injection groups (Figure 3B). The time course of blood meal feeding in female mosquitoes diverged markedly after SK microinjection (Figure 3C). After SK1 or SK2 microinjection at 200 μM (200 pmol in 1 μL), the mosquitoes took significantly longer to complete a blood meal than DEPC water control; SK2 elicited a stronger prolongation than SK1 (Figure 3C). Prolongation by (SK1 + SK2) (at 100 μM final concentration each) was intermediate between SK 1 and SK2 groups (Figure 3C). Note that SK2 mosquitoes (20 mosquitoes) took an average of 98.17 ± 3.40 min to complete

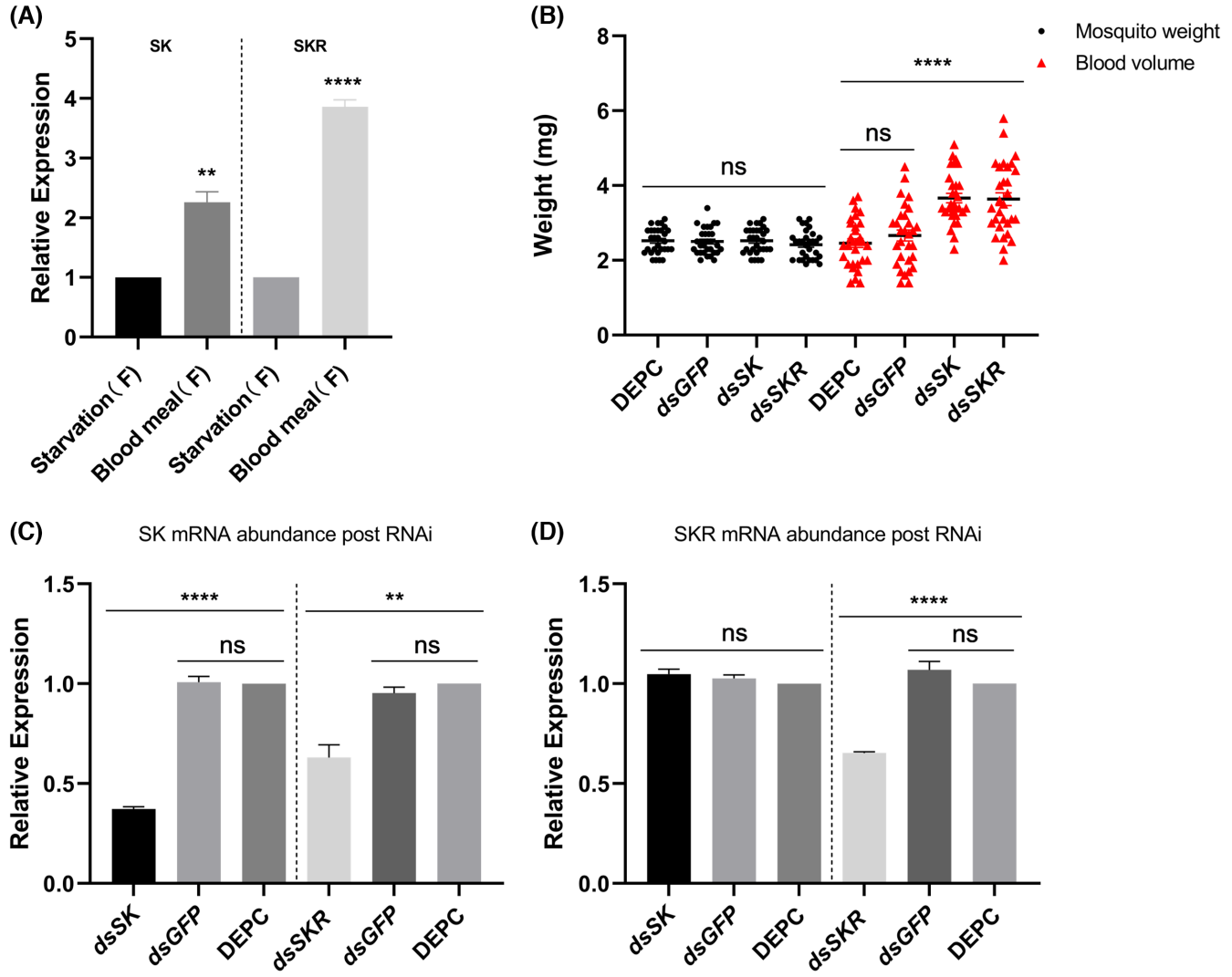

FIGURE 2 Silencing *SK and SKR* genes led to increased size of blood meal in *A. aegypti*. (A) *SK* and *SKR* mRNA levels in the mosquito head before and after a blood meal. The left side is *SK* mRNA in female mosquitoes after starvation and blood sucking, and the right side is *SKR* mRNA in female mosquitoes after starvation and blood meal. $^{**}p = .0020$, $^{****}p < .0001$. (B) Blood meal weight in female mosquitoes with *SK* and *SKR* gene knockdown, 30 female mosquitoes in each experimental group ($N = 30$). $^{****}p < .0001$. (C) The SK mRNA level after *SK* and *SKR* gene knockdown. $^{**}p = .0013$, $^{****}p < .0001$. (D) SKR mRNA level after *SK* and *SKR* gene knockdown. $^{****}p < .0001$. All data are mean ± SEM.

a blood meal, while DEPC water controls (20 mosquitoes) took only 31.50 ± 5.77 min (Figure 3C). At the same concentration, SK1 was significantly less active to prolong feeding. No difference in *SKR* mRNA expression was found between SK-injected experimental groups and DEPC water-injected control (Figure 3D).

The effect of SK2 (at 200 μM) as presented in Figure 3C was also established at lower doses of 50, 100, and 150 μM (Figure 3E). Compared with controls, no significant difference was found in the blood intake of female mosquitoes injected with 50 μM SK2, while blood intake after injection with 100 and 150 μM SK2 was significantly reduced (data with SK2 at 200 μM in panel C replotted in panel E) (right, Figure 3E). Therefore, 100 μM may be the lowest effective concentration of SK2 (right, Figure 3E). Note that no changes in body weight were found with SK2 injections at different doses (left, Figure 3E). A 1:1 mixture of SK2 at 200 μM (200 pmol in 1 μL) and the cholecystokinin antagonist proglumide 28 mM (28.06 nmol in 1 μL) was then injected. The blood intake after this mixed injection was higher compared to the single injection of SK2 at 100 μM (100 pmol in 1 μL), but there was no significant difference compared to the control group of DEPC water, indicating that proglumide reversed effectively the SK2 inhibition (right, Figure 3F). No difference in pre-blood meal body weight was seen among these different groups (left, Figure 3F). To examine the signaling pathway downstream of SKR activation, the receptor gene *SKR* was ectopically expressed in a mammalian cell line widely used for functional expression of GPCR.

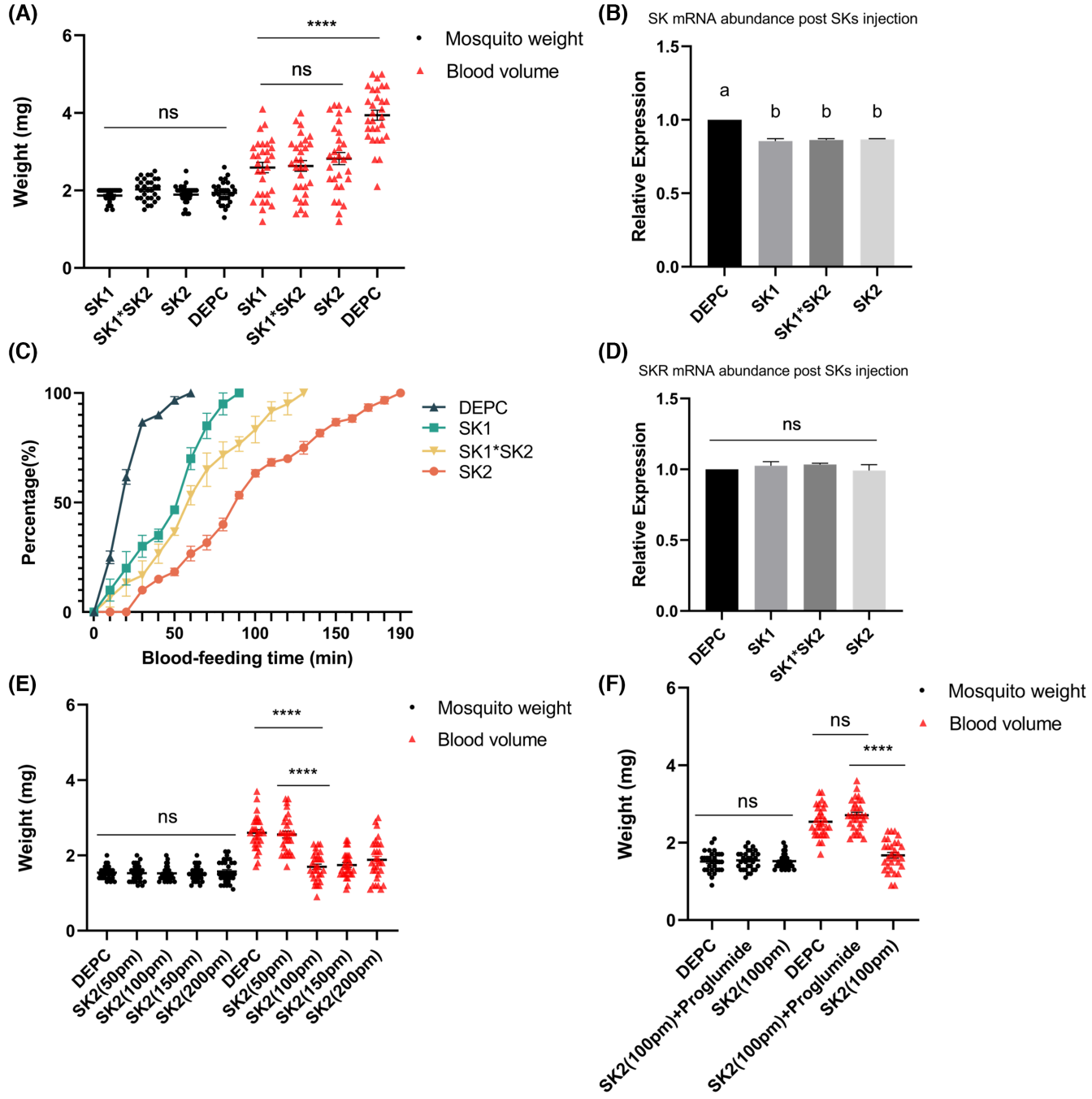

FIGURE 3 Sulfakinin injection reduced and delayed blood meal feeding in female mosquitoes. (A) Blood sizes of female mosquitoes after sulfakinin (SK1, SK2) injection, 30 female mosquitoes in each experimental group. ****$p < .0001$. (B) The SK mRNA levels in mosquito head tissue after SK1, SK1 + SK2, SK2 injection. (C) Effect of SK1 and SK2 injection on blood-feeding time in female mosquitoes. The three experimental groups were SK1 ($N = 20$), SK1 + SK2 ($N = 20$), and SK2 ($N = 20$) injection. Controls were injected with DEPC water ($N = 20$). The number of mosquitoes having finished a blood meal was recorded every 10 min until all mosquitoes had finished blood feeding. The experiment was performed in triplicates. (D) The *SKR* mRNA levels in mosquito head tissue after SK1, SK1 + SK2, SK2, injection. (E) Dose-dependent inhibition of feeding by SK2 injection (pmoles in 1 μL). Blood weights of female mosquitoes after different concentrations of sulfakinin 2 (SK2) injection, 30 female mosquitoes in each experimental group. ****$p < .0001$. (F) Mixed injection of SK2 and cholecystokinin antagonist proglumide. The experimental groups were SK2 (100 pmoles), SK2 (100 pmoles) + proglumide. The control group was DEPC water. 24 h after injection, a blood meal weighing experiment was conducted. ****$p < .0001$. All data are mean ± SEM. Small letters "a, b" in panel (C) denote that significant differences are marked with alphabets a–b, with the same letter indicating no significant difference, while different letters indicate significant differences.

3.4 | Functional expression of the SK receptor gene *SKR*

In perfused, un-transfected parental CHO-K1 cells, the basal calcium level remained stable (Figure 4A) and SK1 stimulation at 30 nM had no effect (Figure 4B). Basal calcium levels remained stable also in un-stimulated SKR-CHO-K1 cells (Figure 4C). Stimulation with SK1 at 300 pM did not elicit any change in calcium levels (Figure 4D) in SKR-CHO-K1 cells but higher concentrations of 1, 3, 10, and 30 nM all induced robust calcium spikes (Figure 4E–H). Quantification of the elicited calcium spikes (area under the peaks above baseline) revealed a monophasic dose–response curve, with a calculated EC_{50} for SK1 of 1.18 nM (Figure 4I). After tagging with a fluorescent protein KillerRed, confocal imaging confirmed localization of SKR in the plasma membrane of SKR-KillerRed-CHO-K1 cells (Figure 4J).

The effect of SK2 stimulation was also examined. In this series of experiments, the parental CHO-K1 cells again showed a stable baseline (Figure 5A). Stimulation with SK2 at 30 nM had no effect on CHO-K1 cells (Figure 5B). Un-stimulated SKR-CHO-K1 cells showed a stable baseline calcium concentration (Figure 5C). SK2 at 100 pM did not stimulate any increases in calcium concentration (Figure 5D), but higher concentrations of 300 pM, 1, 3, 10, and 30 nM all elicited lasting calcium oscillations in SKR-CHO-K1 cells (Figure 5E–I). Quantification of the calcium oscillations (areas under the peak above baseline per 10 min) after SK2 stimulation demonstrated a clear dose–response relationship, with a calculated EC_{50} for SK2 of 251 pM (Figure 5J).

In parallel experiments, we wanted to establish the effect of the mammalian homolog cholecystokinin (CCK). Again, the SKR-CHO-K1 cells in the absence of stimulation showed a stable baseline in calcium levels (Figure 6A). Low CCK at 1 nM had no effect, but at 10 nM and 100 nM CCK elicited clear calcium increases in the SKR-CHO-K1 cells (Figure 6B–D). Millimolar dopamine (1 mM) showed no effect in SKR-CHO-K1 cells (Figure 6E). To demonstrate the difference in efficacy of CCK in stimulating mosquito SKR and mammalian cholecystokinin 1 receptor (CCK1R), rat pancreatic acini were isolated. A stable baseline was observed in isolated rat pancreatic acini in the absence of any simulation (Figure 6F), but a physiological CCK concentration of only 10 pM triggered robust calcium oscillations (Figure 6G). SK2 at 3 nM elicited strong calcium oscillations in SKR-CHO-K1 cells (Figure 6H), but in the presence of the antagonist devazepide 10 nM, SK2 (3 nM) no longer induced any calcium increases (Figure 6I); therefore, the antagonist devazepide (against mammalian CCK1R) was also effective to block mosquito SKR. Quantifications of the calcium responses in these experiments (A–I) are presented in Figure 6J.

4 | DISCUSSION

Female *Aedes aegypti* mosquitoes are normally dependent on blood meals to produce eggs and in the process spread disease-causing arbovirus among human subjects. Here, sulfakinin receptor regulation on *Aedes aegypti* mosquito blood meal intake was investigated. Downregulation of SK and SK receptor (*SK*, *SKR*) expression was found to increase, but microinjection of the SK peptides (SK1, SK2) to decrease blood meal intake. The mammalian CHO-K1 cells expressing the *SKR* gene showed persistent calcium spikes after stimulation with sulfakinin.

SK and *SKR* in *A. aegypti* were found to be highly expressed in the head but only moderately in other tissues (such as thorax, salivary gland, cuticle) (Figure 1). It is interesting to note that *SK* and *SKR* have been found previously to be mainly expressed in the head and midgut in *T. castaneum*, *R. prolixus*, *N. lugens*, and *P. americana (L.)*.[43] *SKR* has been found to be expressed mainly in the head and testis in the silkworm.[24,44] The SKR receptor was found mainly in the midgut in *P. americana (L.)*.[25] RNA-seq data revealed that in the Thai strain of *A. aegypti*, SKR was most abundantly expressed in the ovaries.[45] Those experiments on the Thai strain were, however, performed on mosquitoes 5–12 days after emergence but not fed any blood meal. In the present study, *SK and SKR* were found not highly expressed (when compared with the mosquito head, for example) in the ovaries of the Rockefeller strain of *A. aegypti*, three days after emergence and after blood meals (Figure 1). Both age and blood meal feeding might thus have led to the differences in the expression levels of the *SKR* gene.

The RNAi and SK peptide injection experiments revealed that SK and SKR are important to regulate blood meal intake and satiety in *A. aegypti* (Figures 2 and 3). The effect of SK has been studied before in *D. melanogaster*, *L. migratoria*, *G. bimaculatus*, *P. americana* (L.), and other insect species.[20,22,23,46] In the present work, the blood meal size of female mosquitoes with silenced *SK* and *SKR* genes increased markedly compared with female mosquitoes in control groups (Figure 2). Moreover, SK injection (in the thorax) not only reduced blood intake but also extended the time required for all mosquitoes to complete blood feeding (Figure 3). Both SK peptides in *A. aegypti* thus function as satiety factors that decrease the appetite. Note particularly that the time required for all mosquitoes to complete blood feeding after SK injection increased from 31.50 ± 5.77 min to 50.83 ± 5.97, 66.33 ± 3.06, and 98.17 ± 3.40 with SK1, SK1 + SK2, and SK2 injections, respectively (Figure 3). SK2 was found more effective than SK1 (Figure 3); this was corroborated in functionally expressed SKR in CHO-K1 cells (Figure 6). SK2 inhibition of feeding, for example, was clearly dose-dependent (Figure 3). The receptor antagonist proglumide reversed

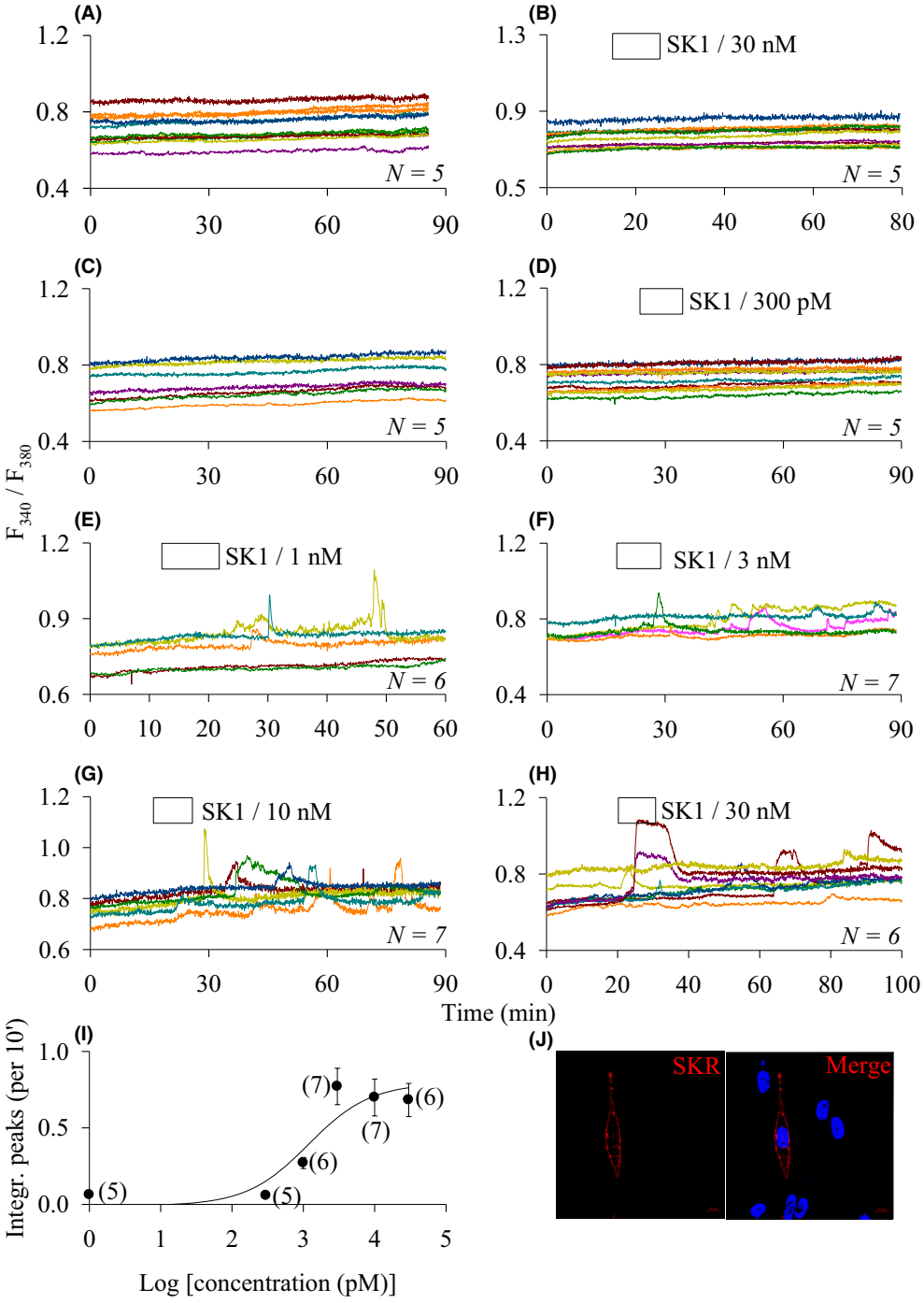

FIGURE 4 SK1 triggered persistent cytosolic calcium spikes in SKR-CHO-K1 cells Fura-2-loaded CHO-K1 (A, B) or SKR-CHO-K1 cells (C–H) were perifused, SK1 of 0 (A, C), 300 pM (D), 1 nM (E), 3 nM (F), 10 nM (G), 30 nM (B, H) was added as indicated. (I) Quantitative analysis of calcium peak areas above baseline (per 10 min) from multiple experiments (number shown in brackets at each data point), with typical calcium traces shown in panels (C–H), is summarized (I) ($N = 5$–7). $EC_{50} = 1.18$ nM. The abscissa in panels (A–H) is time in min. (J) Confocal image of sulfakinin receptor tagged at the N-terminal with KillerRed (red), and counterstained with nuclear dye DAPI (blue). KillerRed: λ_{ex}, 561 nm, λ_{em} 618 nm; DAPI—λ_{ex} 405 nm, λ_{em} 477 nm. Scale bar: 10 μm. Images were obtained from a laser scanning confocal microscope (Zeiss LSM 710).

the feeding inhibition of SK2 in mosquitoes (Figure 3) at a dose similar to those used in mice and zebrafish.[47–50]

SK injection in the thorax not only reduced food intake but also extended the time required for the mosquitoes to complete blood feeding (Figure 3). In regard to the delayed time course of blood meal intake, we are unable in the present work to actually distinguish between possible changes in the food-probing behavior or the rate at which

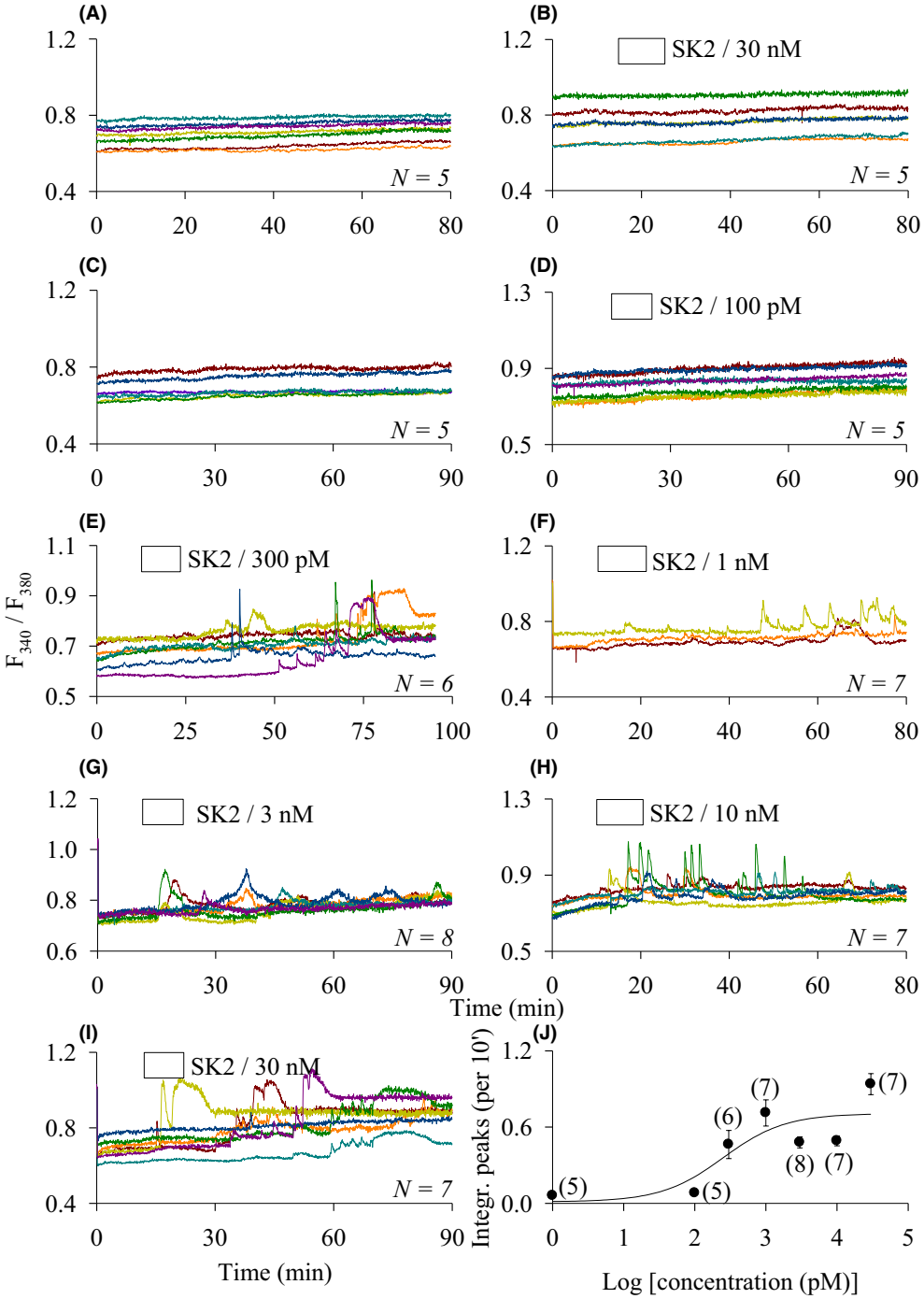

FIGURE 5 SK2 triggered persistent cytosolic calcium spikes in SKR-CHO-K1 cells Fura-2-loaded CHO-K1 (A, B) or SKR-CHO-K1 cells (C–I) were perifused, SK2 of 0 (A, C), 100 pM (D), 300 pM (E), 1 nM (F), 3 nM (G), 10 nM (H), 30 nM (B, I) was added as indicated. (J) Quantitative analysis of calcium peak areas above baseline (per 10 min) from multiple experiments (number shown in brackets), with typical calcium traces shown in (C–I), was plotted in (J) ($N = 5$–8). $EC_{50} = 251$ pM. The abscissa in panels (A–I) is time in min as indicated.

the female mosquitoes were satiated. In future studies, more attention should be paid to differentiate these two possibilities. After injection, the SK peptides would probably diffuse directly to sensory nerve endings or via the lymphatic/circulatory systems to target neurons in the periphery, eventually sending anti-feeding signals to the CNS. Recently, it has been found that SKR is widely expressed in the CNS, predominantly in neuronal cells of *Drosophila melanogaster*.[51] The *Drosophila* SK peptide was transported downward from the MPl medial neurosecretory cells with projections extending down the ventral ganglion.[52] The activation of this inhibitory feeding circuit is likely to last for some time before the SK is finally metabolized and the inhibition wanes. An antagonist

such as proglumide likely exerts its receptor-blocking effect also in the periphery, at the sensory neurons. This notion will, however, need verification in future studies of the detailed distribution of SKR-expressing sensory neurons.

SK signaling and its effect on feeding might be quite complex. In *D. melanogaster*, SK peptides are released from neurons to modulate diverse functions such as stress, exercise, metabolism, feeding, mating, and aggression.[14,31,53] In other insects such as *O. arenosella* (Walk.), *P. americana*, and *R. prolixus*, beyond inhibiting food intake, SK peptides also stimulate secretion of digestive enzymes[54] and muscle contraction.[17] In our present study, spatiotemporal expression profiles (Figure 1) revealed that both *SK* and *SKR* genes are expressed in different tissues and in different development stages (Figure 1), and are likely involved in the regulation of physiological functions related to feeding.

Insect feeding is known to be regulated not only by the sulfakinin receptors but also by dopamine receptors.[55] Hunger also increases dopamine concentration in the brain of foraging bees; when dopamine signaling is inhibited, foraging time increases.[55] In *C. elegans*, release of SK and dopaminergic regulation of motor circuit activity is at the core of food search behavior. *C. elegans* behavior is regulated by food-related sensory input in this conserved dopamine-SK signaling pathway.[56] Dopamine itself, however, does not seem to have any direct effect on the *Aedes aegyptii* SKR receptor, at least when expressed ectopically in the mammalian cell line CHO-K1 (Figure 6). Note that even millimolar dopamine concentration did not have any effect on SKR-CHO-K1 cells (Figure 6).

Heterologous expression of the *SKR* gene in CHO-K1 cells showed that both SK1 (Figure 4) and SK2 (Figure 5) could stimulate the heterologously expressed SKR receptor. SKR-CHO-K1 cells were more responsive to SK2 than SK1, with EC_{50} of 251 pM (SK2) and 1.18 nM (SK1), respectively (Figs. 4, 5). The sulfakinin effect was found blocked by the receptor antagonist devazepide (Figure 6). The mammalian peptide cholecystokinin (CCK) was also able to be activate the mosquito sulfakinin receptor (SKR) dose dependently, but probably less efficiently than the mosquito peptide SK2 (Figure 6). In contrast, CCK was much more efficacious to activate the mammalian receptor (CCK1R) present in rat pancreatic acini (Figure 6). Also note that cholecystokinin stimulation was readily washed out in perifused SKR-CHO-K1 cells (Figure 6), but SK-elicited cytosolic calcium oscillations showed a significant lag time already at lower concentrations (Figures 4 and 5) and the stimulation was long-lasting even after wash-out (Figures 4–6). It would be interesting to elucidate the molecular mechanisms underlying such differences in future studies.

The lasting effects of both SK1 and SK2 to induce calcium spikes are rather similar to the permanent photodynamic activation of the CCK1 receptor (CCK1R) in mammalian and avian pancreatic acini, and in ectopically expressed CCK1R in HEK293 cells.[37–41] Agonist-stimulated SKR activation in *A. aegypti* resembles photodynamic CCK1 receptor activation in mammalian and avian pancreatic acini.[41] Long-lasting activation of G protein-coupled CCK or CCK-like (SK) receptors might be an evolutionarily conserved property of this particular member of the rhodopsin-like or A class GPCR. Although the detailed reasons for SKR activation-induced persistent calcium spikes are not known at the present, more insights could be gained from receptor single-molecule force spectroscopy[57] and super-resolution microscopy[58–60] studies in the future.

In conclusion, the *SK* and *SKR* genes were identified from the *A. aegypti* genome and their spatiotemporal expression profiles established. RNAi knockdown and SK microinjection experiments, as well as antagonist reversal of agonist inhibition of feeding in vivo, provide strong evidence that SK peptides inhibit mosquito blood feeding. In vitro experiments confirmed the Gq-coupling or calcium-mobilizing property of the sulfakinin receptor. The wide distribution of *SK* and *SKR* genes over all developmental stages and in multiple tissues in *A. aegypti* highlights their importance in regulating feeding and related behaviors. Although it is now established that the sulfakinin–sulfakinin receptor system inhibits female *A. aegypti* mosquito blood meal intake, there may be still a long way to go before a selective insecticide targeting *A. aegypti* mosquito blood-feeding physiology could be available. More studies must be done in the future, possibly in the following directions. (1) Development of *A. aegypti* mosquito-selective agonists. We know from the present work that the mammalian peptide cholecystokinin (CCK) has much higher efficacy/sensitivity for the rat pancreatic acinar cell receptor in comparison with the mosquito sulfakinin receptor (a difference of three orders of magnitude, see Figure 6), and reverse selectivity for the mosquito receptor is highly desired. (2) In the present work, mosquitoes at three days after eclosion are studied, sulfakinin receptor physiology at later stages of mosquito adult life may need to be examined. In vivo studies of the activation of the mosquito receptor in the brain or elsewhere (such as by fluorescent calcium imaging) will need to be done. (3) Sulfakinin receptor structural biology. The structures of mosquito sulfakinin receptor and lower vertebrate receptors need to be solved. Receptor structural works will help to search for an effective drug-binding site for selective insecticide. In this regard, high throughput screening of novel small

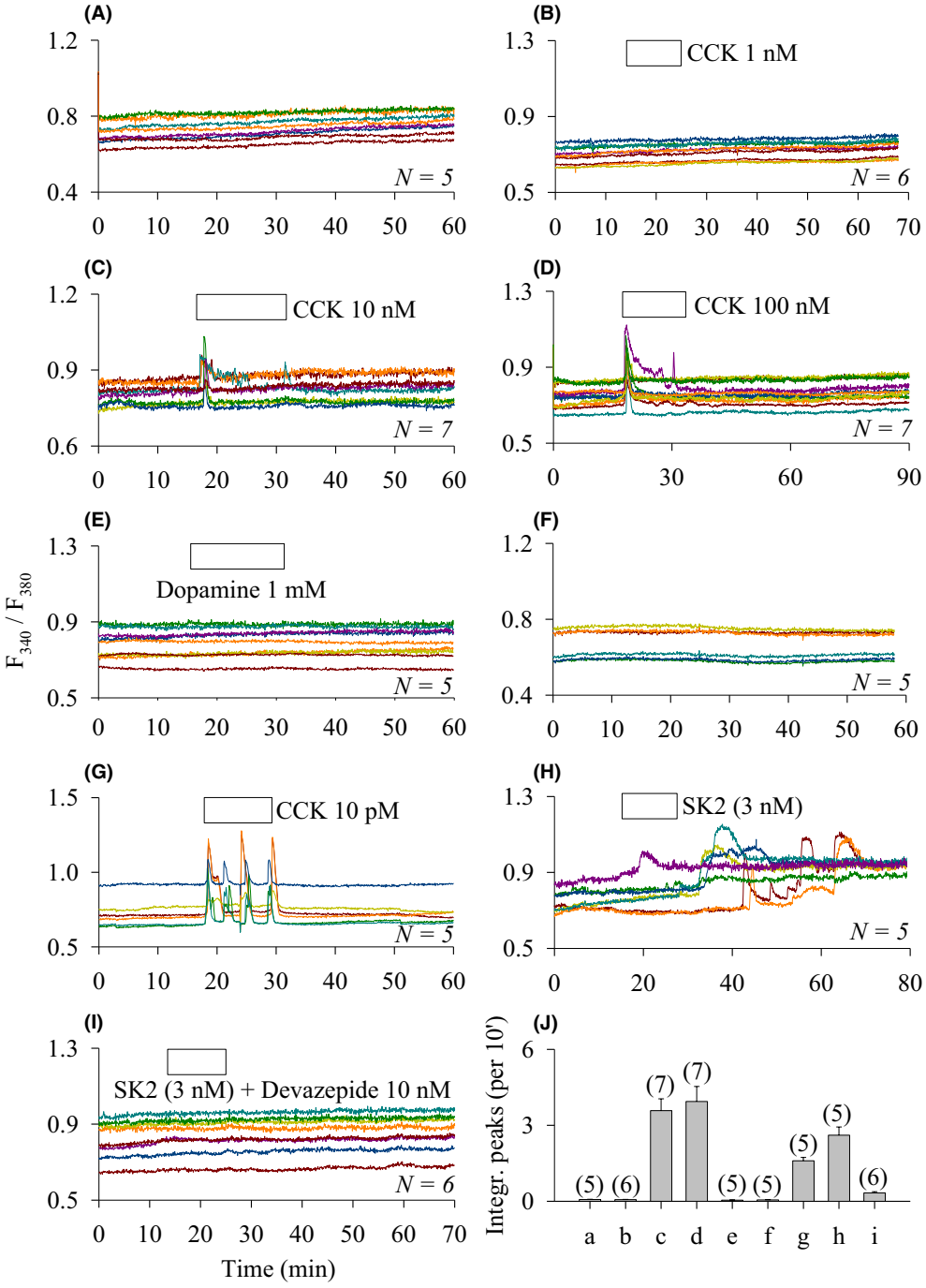

FIGURE 6 SKR was responsive to the mammalian peptide cholecystokinin (CCK), but not to dopamine in SKR-CHO-K1 cells Fura-2-loaded SKR-CHO-K1 cells (A–E, H, I), or rat pancreatic acini (F, G), were perifused, with buffer alone (A, F), or with CCK 1 nM (B),10 nM (C), 100 nM (D), or dopamine 1 mM (E), as indicated. The isolated rat pancreatic acini were perifused with buffer alone (F), or with CCK 10 pM (G). In parallel experiments, SK2 (3 nM, H) alone, or with SK2 (3 nM) + devazepide 10 nM (I) were added to perifused SKR-CHO-K1 cells. The abscissa in panels (A–I) are time in min. (J) Quantification of calcium peak areas (area under the curve above baseline, per 10 min) or lack of it in corresponding time period from multiple independent experiments ($N = 5–7$, as shown in brackets), with typical calcium traces as shown in panels (A–I), as marked at the bottom of each column in panel (J).

molecules targeting the mosquito sulfakinin receptor will be helpful. (4) The mammalian cholecystokinin receptor is known to be permanently activated by photodynamic action (see the paragraph immediately above), permanent photodynamic activation of the mosquito sulfakinin receptor in vivo, when possible, might serve to keep the mosquito at a constantly satiated state therefore refrain from blood meal intake, to inhibit mosquito egg maturation/reproduction and transmission of the arbovirus among humans.

AUTHOR CONTRIBUTIONS

Qian Han and Zong Jie Cui conceived the idea of the project, secured funding, supervised the project, and wrote the final version of the manuscript. Qian Han and Zong Jie Cui designed the study. Linlong Jiang, Xiao Bing Xie, Lei Zhang, Yu Tang, Xiaojing Zhu, and Yue Hong contributed to material preparation, data collection, and analysis. LJ and Xiao Bing Xie wrote the initial drafts of the manuscript and Qian Han, and Zong Jie Cui and Bill S. Hansson revised the manuscript. All authors agreed to the submitted version of the manuscript. Linlong Jiang, Lei Zhang, Yu Tang, Xiaojing Zhu, Yue Hong, Bill S. Hansson, and Qian Han obtained the primary data in Figures 1–3. Xiao Bing Xie and Zong Jie Cui obtained the primary data in Figures 4–6.

ACKNOWLEDGMENTS

This work was supported by grants from the Natural Science Foundation of China (32271278, U22A20363, 31971170), the Hainan Province Science and Technology Special Fund (ZDKJ2021035), and the National High-end Foreign Experts Recruitment Plan (G2021034003L).

DISCLOSURES

The authors have no relevant financial or non-financial interests to disclose.

DATA AVAILABILITY STATEMENT

All data are contained in the article.

ANIMAL USE ETHICS APPROVAL

The animal protocol used in this work to isolate pancreatic acini from male rats was approved by The Animal Use and Ethics Committee, College for Life Sciences, Beijing Normal University (No. CLS-EAW-2017-015). Only male rats were used to isolate the pancreatic acini, in order to rule out any possible interference of the sex cycle on the function of the isolated rat pancreatic acini.

ORCID

Bill S. Hansson https://orcid.org/0000-0002-4811-1223
Zong Jie Cui https://orcid.org/0000-0003-4252-4876
Qian Han https://orcid.org/0000-0001-6245-5252

REFERENCES

1. Lwande OW, Obanda V, Lindström A, et al. Globe-trotting *Aedes aegypti* and *Aedes albopictus*: risk factors for arbovirus pandemics. *Vector Borne Zoonotic Dis*. 2020;20:71-81. doi:10.1089/vbz.2019.2486
2. Gan SJ, Leong YQ, Bin Barhanuddin MFH, et al. Dengue fever and insecticide resistance in *Aedes* mosquitoes in Southeast Asia: a review. *Parasit Vectors*. 2021;14:315. doi:10.1186/s13071-021-04785-4
3. Li M, Kandul NP, Sun R, et al. Targeting sex determination to suppress mosquito populations. *elife*. 2024;12:RP90199. doi:10.7554/eLife.90199
4. Carrasco D, Lefèvre T, Moiroux N, Pennetier C, Chandre F, Cohuet A. Behavioural adaptations of mosquito vectors to insecticide control. *Curr Opin Insect Sci*. 2019;34:48-54. doi:10.1016/j.cois.2019.03.005
5. Christophers SR. *Aedes aegypti (L.) the Yellow Fever Mosquito: its Life History, Bionomics and Structure*. Cambridge University Press; 2009.
6. Trpis M. Autogeny in diverse populations of *Aedes aegypti* from East Africa. *Tropenmed Parasitol*. 1977;28:77-82.
7. Isoe J, Simington CJ, Oscherwitz ME, et al. Characterization of essential eggshell proteins from *Aedes aegypti* mosquitoes. *BMC Biol*. 2023;21:214. doi:10.1186/s12915-023-01721-z
8. Marinotti O, Ngo T, Kojin BB, et al. Integrated proteomic and transcriptomic analysis of the *Aedes aegypti* eggshell. *BMC Dev Biol*. 2014;14:15. doi:10.1186/1471-213X-14-15
9. Farnesi LC, Vargas HCM, Valle D, Rezende GL. Darker eggs of mosquitoes resist more to dry conditions: melanin enhances serosal cuticle contribution in egg resistance to desiccation in *Aedes*, *anopheles* and *Culex* vectors. *PLoS Negl Trop Dis*. 2017;11:e0006063. doi:10.1371/journal.pntd.0006063
10. East PD, Hales DF, Cooper PD. Distribution of sulfakinin-like peptides in the central and sympathetic nervous system of the American cockroach, *Periplaneta americana* (L.) and the field cricket, *Teleogryllus commodus* (Walker). *Tissue Cell*. 1997;29:347-354. doi:10.1016/s0040-8166(97)80010-9
11. Guo D, Zhang S, Zhang Y-J, Ma J-Y, Gao C-F, Wu S-F. Sulfakinin inhibits activity of digestive enzymes in the brown planthopper, *Nilaparvata lugens*. *J Asia Pac Entomol*. 2020;23:1073-1082. doi:10.1016/j.aspen.2020.09.004
12. Guo Z, He X, Jiang C, Shi Y, Zhou N. Activation of *Bombyx mori* neuropeptide G protein-coupled receptor A19 by neuropeptide RYamides couples to G(q) protein-dependent signaling pathways. *J Cell Biochem*. 2021;122:456-471. doi:10.1002/jcb.29874
13. Wei B, Nachman RJ, Goldsworthy V, De Loof A. Schoofs. Sulfakinins reduce food intake in the desert locust, *Schistocerca gregaria*. *J Insect Physiol*. 2000;46:1259-1265. doi:10.1016/s0022-1910(00)00046-9
14. Wu S, Guo C, Zhao H, et al. Drosulfakinin signaling in fruitless circuitry antagonizes P1 neurons to regulate sexual arousal in *Drosophila*. *Nat Commun*. 2019;10:4770. doi:10.1038/s41467-019-12758-6
15. Al-Alkawi H, Lange AB, Orchard I. Cloning, localization, and physiological effects of sulfakinin in the kissing bug, *Rhodnius prolixus*. *Peptides*. 2017;98:15-22. doi:10.1016/j.peptides.2016.12.017
16. Koziol U. Precursors of neuropeptides and peptide hormones in the genomes of tardigrades. *Gen Comp Endocrinol*. 2018;267:116-127. doi:10.1016/j.ygcen.2018.06.012
17. Zels S, Dillen S, Crabbe K, Spit J, Nachman RJ, Broeck JV. Sulfakinin is an important regulator of digestive processes in the migratory locust, *Locusta migratoria*. *Insect Biochem Mol Biol*. 2015;61:8-16. doi:10.1016/j.ibmb.2015.03.008
18. Williams MJ, Goergen P, Rajendran J, et al. Obesity-linked homologues TfAP-2 and Twz establish meal frequency in *Drosophila melanogaster*. *PLoS Genet*. 2014;10:e1004499. doi:10.1371/journal.pgen.1004499
19. Nichols R, Egle JP, Langan NR, Palmer GC. The different effects of structurally related sulfakinins on *Drosophila melanogaster* odor preference and locomotion suggest involvement of

distinct mechanisms. *Peptides*. 2008;29:2128-2135. doi:10.1016/j.peptides.2008.08.010

20. Kubiak TM, Larsen MJ, Burton KJ, et al. Cloning and functional expression of the first *Drosophila melanogaster* sulfakinin receptor DSK-R1. *Biochem Biophys Res Commun*. 2002;291:313-320. doi:10.1006/bbrc.2002.6459
21. Lin X, Yu N, Smagghe G. Insulin receptor regulates food intake through sulfakinin signaling in the red flour beetle, *Tribolium castaneum*. *Peptides*. 2016;80:89-95. doi:10.1016/j.peptides.2016.03.002
22. Maestro JL, Aguilar R, Pascual N, et al. Screening of antifeedant activity in brain extracts led to the identification of sulfakinin as a satiety promoter in the German cockroach. Are arthropod sulfakinins homologous to vertebrate gastrins-cholecystokinins? *Eur J Biochem*. 2001;268:5824-5830. doi:10.1046/j.0014-2956.2001.02527.x
23. Meyering-Vos M, Muller A. RNA interference suggests sulfakinins as satiety effectors in the cricket *Gryllus bimaculatus*. *J Insect Physiol*. 2007;53:840-848. doi:10.1016/j.jinsphys.2007.04.003
24. Slocinska M, Chowanski S, Marciniak P. Identification of sulfakinin receptors (SKR) in *Tenebrio molitor* beetle and the influence of sulfakinins on carbohydrates metabolism. *J Comp Physiol B-Biochem Syst Environ Physiol*. 2020;190:669-679. doi:10.1007/s00360-020-01300-6
25. Nachman RJ, Holman GM, Haddon WF, Ling N. Leucosulfakinin, a sulfated insect neuropeptide with homology to gastrin and cholecystokinin. *Science (New York, NY)*. 1986;234:71-73. doi:10.1126/science.3749893
26. Nachman RJ, Holman GM, Cook BJ, Haddon WF, Ling N. Leucosulfakinin-II, a blocked sulfated insect neuropeptide with homology to cholecystokinin and gastrin. *Biochem Biophys Res Commun*. 1986;140:357-364. doi:10.1016/0006-291x(86)91098-3
27. Nichols R, Schneuwly SA, Dixon JE. Identification and characterization of a *Drosophila* homologue to the vertebrate neuropeptide cholecystokinin. *J Biol Chem*. 1988;263:12167-12170.
28. Nassel DR, Wu S-F. Cholecystokinin/sulfakinin peptide signaling: conserved roles at the intersection between feeding, mating and aggression. *Cell Mol Life Sci*. 2022;79:188. doi:10.1007/s00018-022-04214-4
29. Agrawal P, Kao D, Chung P, Looger LL. The neuropeptide drosulfakinin regulates social isolation-induced aggression in *Drosophila*. *J Exp Biol*. 2020;223:jeb207407. doi:10.1242/jeb.207407
30. Nichols R, Bass C, Katanski C. Structure-activity relationship data and ligand-receptor interactions identify novel agonists consistent with sulfakinin tissue-specific signaling in *Drosophila melanogaster* heart. *Front Biosci-Landmark*. 2022;27:150. doi:10.31083/j.fbl2705150
31. Wang T, Jing B, Deng B, et al. Drosulfakinin signaling modulates female sexual receptivity in *Drosophila*. *elife*. 2022;11:e76025. doi:10.7554/eLife.76025
32. Bloom M, Lange AB, Orchard I. Identification, functional characterization, and pharmacological analysis of two sulfakinin receptors in the medically-important insect *Rhodnius prolixus*. *Sci Rep*. 2019;9:13437. doi:10.1038/s41598-019-49790-x
33. Zhang L, Tang Y, Chen H, et al. Arylalkalamine N-acetyltransferase-1 acts on a secondary amine in the yellow fever mosquito, *Aedes aegypti*. *FEBS Lett*. 2022;596:1081-1091. doi:10.1002/1873-3468.14316
34. Livak KJ, Schmittgen TD. Analysis of relative gene expression data using real-time quantitative PCR and the $2^{-\Delta\Delta Ct}$ method. *Methods (San Diego, Calif)*. 2001;25:402-408. doi:10.1006/meth.2001.1262
35. Chen J, Lu HR, Zhang L, Liao CH, Han Q. RNA interference-mediated knockdown of 3, 4-dihydroxyphenylacetaldehyde synthase affects larval development and adult survival in the mosquito *Aedes aegypti*. *Parasit Vectors*. 2019;12:311-322. doi:10.1186/s13071-019-3568-7
36. Zhang L, Li M-Z, Chen Z-H, Tang Y, Liao C-H, Han Q. Arylalkalamine N-acetyltransferase-1 functions on cuticle pigmentation in the yellow fever mosquito, *Aedes aegypti*. *Insect Sci*. 2021;28:1591-1600. doi:10.1111/1744-7917.12895
37. Cui ZJ, Kanno T. Photodynamic triggering of calcium oscillation in the isolated rat pancreatic acini. *J Physiol*. 1997;504:47-55. doi:10.1111/j.1469-7793.1997.047bf.x
38. An YP, Xiao R, Cui H, Cui ZJ. Selective activation by photodynamic action of cholecystokinin receptor in the freshly isolated rat pancreatic acini. *Br J Pharmacol*. 2003;139:872-880. doi:10.1038/sj.bjp.0705295
39. Jiang WY, Li Y, Li ZY, Cui ZJ. Permanent photodynamic cholecystokinin 1 receptor activation: dimer-to-monomer conversion. *Cell Mol Neurobiol*. 2018;38:1283-1292. doi:10.1007/s10571-018-0596-3
40. Jiang HN, Li Y, Jiang WY, Cui ZJ. Cholecystokinin 1 receptor—a unique G protein-coupled receptor activated by singlet oxygen (GPCR-ABSO). *Front Physiol*. 2018;9:497. doi:10.3389/fphys.2018.00497
41. Wang J, Cui ZJ. Photodynamic activation of cholecystokinin 1 receptor is conserved in mammalian and avian pancreatic acini. *Biomedicine*. 2023;11:885. doi:10.3390/biomedicines11030885
42. Li Y, Cui ZJ. Transmembrane domain 3 is a transplantable pharmacophore in the photodynamic activation of cholecystokinin 1 receptor. *ACS Pharmacol Transl Sci*. 2022;5:539-547. doi:10.1021/acsptsci.2c00031
43. Chen X, Peterson J, Nachman RJ, Ganetzky B. Drosulfakinin activates CCKLR-17D1 and promotes larval locomotion and escape response in *Drosophila*. *Fly*. 2012;6:290-297. doi:10.4161/fly.21534
44. Yu N, Nachman RJ, Smagghe G. Characterization of sulfakinin and sulfakinin receptor and their roles in food intake in the red flour beetle *Tribolium castaneum*. *Gen Comp Endocrinol*. 2013;188:196-203. doi:10.1016/j.ygcen.2013.03.006
45. Hixson B, Bing XL, Yang X, Bonfini A, Nagy P, Buchon N. A transcriptomic atlas of *Aedes aegypti* reveals detailed functional organization of major body parts and gut regional specializations in sugar-fed and blood-fed adult females. *elife*. 2022;11:e76132. doi:10.7554/eLife.76132
46. Caers J, Verlinden H, Zels S, Vandersmissen HP, Vuerinckx K, Schoofs L. More than two decades of research on insect neuropeptide GPCRs: an overview. *Front Endocrinol*. 2012;3:151. doi:10.3389/fendo.2012.00151
47. Hahne W, Jensen R, Lemp G, Gardner J. Proglumide and benzotript: members of a different class of cholecystokinin receptor antagonists. *Proc Natl Acad Sci USA*. 1981;78:6304-6308. doi:10.1073/pnas.78.10.6304
48. Niederau C, Ferrell L, Grendell J. Caerulein-induced acute necrotizing pancreatitis in mice: protective effects of proglumide,

benzotript, and secretin. *Gastroenterology*. 1985;88:1192-1204. doi:10.1016/s0016-5085(85)80079-2
49. Gay M, Safronenka A, Cao H, et al. Targeting the cholecystokinin receptor: a novel approach for treatment and prevention of hepatocellular cancer. *Cancer Prev Res (Philadelphia, PA)*. 2021;14:17-30. doi:10.1158/1940-6207.Capr-20-0220
50. Malchiodi Z, Cao H, Gay M, et al. Cholecystokinin receptor antagonist improves efficacy of chemotherapy in murine models of pancreatic cancer by altering the tumor microenvironment. *Cancer*. 2021;13:4949. doi:10.3390/cancers13194949
51. Oikawa I, Kondo S, Hashimoto K, et al. A descending inhibitory mechanism of nociception mediated by an evolutionarily conserved neuropeptide system in *Drosophila*. *elife*. 2023;12:e85760. doi:10.7554/eLife.85760
52. Nichols R. Isolation and expression of the *Drosophila* drosulfakinin neural peptide gene product, DSK-I. *Mol Cell Neurosci*. 1992;3:342-347. doi:10.1016/1044-7431(92)90031-V
53. Zandawala M, Yurgel ME, Texada MJ, et al. Modulation of *Drosophila* post-feeding physiology and behavior by the neuropeptide leucokinin. *PLoS Genet*. 2018;14:e1007767. doi:10.1371/journal.pgen.1007767
54. Harshini S, Nachman RJ, Sreekumar S. In vitro release of digestive enzymes by FMRF amide related neuropeptides and analogues in the lepidopteran insect *Opisina arenosella* (Walk.). *Peptides*. 2002;23:1759-1763. doi:10.1016/s0196-9781(02)00152-3
55. Huang J, Zhang Z, Feng W, et al. Food wanting is mediated by transient activation of dopaminergic signaling in the honey bee brain. *Science*. 2022;376:508-512. doi:10.1126/science.abn9920
56. Bhattacharya R, Touroutine D, Barbagallo B, et al. A conserved dopamine-cholecystokinin signaling pathway shapes context-dependent *Caenorhabditis elegans* behavior. *PLoS Genet*. 2014;10:e1004584. doi:10.1371/journal.pgen.1004584
57. An C, Chen W. Multiplexed single-molecule force spectroscopy for dissecting biophysical regulation of membrane receptors functions on live cells. *Biophys Rep*. 2021;7:377-383.
58. Zhang ML, Ti HY, Wang PY, Li H. Intracellular transport dynamics revealed by single-particle tracking. *Biophys Rep*. 2021;7:413-427.
59. Wang S, Qiao C, Jiang A, Li D, Li D. Instant multicolor super-resolution microscopy with deep convolutional neural network. *Biophys Rep*. 2021;7:304-312.
60. Ye X, Guan M, Guo Y, et al. Live-cell super-resolution imaging unconventional dynamics and assemblies of nuclear pore complexes. *Biophys Rep*. 2023;9:206-214. doi:10.52601/bpr.2023.230010

How to cite this article: Jiang L, Xie XB, Zhang L, et al. Activation of the G protein-coupled sulfakinin receptor inhibits blood meal intake in the mosquito *Aedes aegypti*. *The FASEB Journal*. 2024;38:e23864. doi:10.1096/fj.202401165R